Protein Science (1995), *4*:703–715. Cambridge University Press. Printed in the USA.

Theoretical analysis of the structure of the peptide fasciculin and its docking to acetylcholinesterase

HARALD K.L. VAN DEN BORN,[1,3] ZORAN RADIĆ,[1,5] PASCALE MARCHOT,[1,4] PALMER TAYLOR,[1] AND IGOR TSIGELNY[1,2]

[1] Department of Pharmacology, University of California at San Diego, La Jolla, California 92093-0636
[2] Department of Chemistry and Biochemistry, University of California at San Diego, La Jolla, California 92093-0636

(RECEIVED December 5, 1994; ACCEPTED January 20, 1995)

Abstract

The fasciculins are a family of closely related peptides that are isolated from the venom of mambas and exert their toxic action by inhibiting acetylcholinesterase (AChE). Fasciculins belong to the structural family of three-fingered toxins from Elapidae snake venoms, which include the α-neurotoxins that block the nicotinic acetylcholine receptor and the cardiotoxins that interact with cell membranes. The features unique to the known primary and tertiary structures of the fasciculin molecule were analyzed. Loop I contains an arginine at position 11, which is found only in the fasciculins and could form a pivotal anchoring point to AChE. Loop II contains five cationic residues near its tip, which are partly charge-compensated by anionic side chains in loop III. By contrast, the other three-fingered toxins show full charge compensation within loop II. The interaction of fasciculin with the recognition site on acetylcholinesterase was investigated by estimating a precollision orientation followed by determination of the buried surface area of the most probable complexes formed, the electrostatic field contours, and the detailed topography of the interaction surface. This approach has led to testable models for the orientation and site of bound fasciculin.

Keywords: acetylcholinesterase; elapid peptides; electrostatic fields; fasciculin; snake toxins

The fasciculins are 6,800-Da peptides found in the venom of snakes from the mamba family. The isolated peptides have been shown to be potent inhibitors of acetylcholinesterase (AChE) (Karlsson et al., 1984). Four fasciculins have been described to date: fasciculin 1 (Fas1) and fasciculin 2 (Fas2) from *Dendroaspis angusticeps* (eastern green mamba), toxin C from *Dendroaspis polylepis* (black mamba), and fasciculin 3 (Fas3) from *Dendroaspis viridis*. Their primary structures are known (Karlsson et al., 1985). Fas3 and toxin C were found to have identical primary structures (Marchot et al., 1993). All three fasciculin structures contain 61 amino acids and differ only by one to three residues. So far only the crystal structure of Fas1 has been solved (Kinemage 1; le Du et al., 1992). These peptides fall into a larger family of small three-fingered peptide toxins from Elapidae snake venoms; other members of this family are the cardiotoxins, which interact with cell membranes, and the α-neurotoxins, such as erabutoxin (Ebt) and α-bungarotoxin (Bgt), which are antagonists at the acetylcholine receptor (Karlsson et al., 1984; Endo & Tamiya, 1991).

The fasciculins inhibit AChE of mammals and fish with dissociation constants between 0.4 and 100 pM; the fasciculin–AChE complex, as measured with Fas1 and Fas3, has an extremely slow rate of dissociation, with half times of several hours. Fasciculins are also selective in their action because avian, insect, and snake AChEs are relatively resistant to them and micromolar concentrations are required to inhibit butyrylcholinesterases (BuChEs) from mammals (Karlsson et al., 1984; Cervenansky et al., 1991; Radić et al., 1994). Fas1 and Fas2 have nearly equivalent dissociation constants, whereas Fas3 has a 10-fold lower dissociation constant for rat brain AChE (Marchot et al., 1993).

Recent studies show that Fas3 binds to diisopropylfluorophosphate (DFP)-inhibited enzyme, and that DFP can still enter the active center gorge of the Fas3–AChE complex (Marchot et al., 1993). Moreover, peripheral site inhibitors such as propidium (Taylor & Lappi, 1975), and not active center inhibitors, are competitive with the binding of fasciculins (Karlsson et al., 1984; Marchot et al., 1993). Thus, fasciculin appears to influence AChE catalysis in an allosteric fashion. Indeed, modification of residues residing at the rim of the active center gorge and not residues at the substrate binding site markedly influences fas-

Reprint requests to: Igor Tsigelny, Department of Chemistry and Biochemistry, 0654, University of California at San Diego, 9500 Gilman Drive, La Jolla, California 92093-0654; e-mail: itsigeln@ucsd.edu.

[3] Visiting Scholar, Utrecht University, Faculty of Pharmacy, Utrecht, The Netherlands.

[4] Visiting Scholar, CNRS Unité de Recherche Associée 1455, Université d'Aix-Marseille II, Faculté de Médecine Secteur Nord, Marseille, France.

[5] Visiting Scholar, Institute for Medical Research and Occupational Health, University of Zagreb, Croatia.

ciculin binding (Radić et al., 1994). Hence, fasciculin inhibition could arise both from a gating influence, therein restricting substrate entry into active center gorge and from exerting allosteric control over the commitment to catalysis of the bound substrate.

The availability of the three-dimensional structure of AChE from *Torpedo californica* (Sussman et al., 1991) provides the first structure of the target site for the family of three-fingered Elapidae toxins and has prompted renewed interest in studying the highly selective interactions between this family of toxins and their binding sites. In this study we detail the structure of the fasciculins in relation to related toxins in order to delineate features responsible for their specificity for the AChEs. Secondly, we analyze fasciculin interaction with the peripheral site on AChE by procedures that initially establish a precollision orientation and subsequently analyze probable complexes on the bases of electrostatic forces, surface area of contact, and surface topography of the respective molecules.

Results

Electrostatic properties of the toxins deduced from their three-dimensional structures

Internal structure stabilization

The complete structural maps of Fas1 (le Du et al., 1992) and Ebt-b (Smith et al., 1988) obtained from their crystal coordinates are presented in Figure 1A and B. Figure 1C and D shows only the regions of Fas2 and Fas3 that differ from Fas1. The overall folding of fasciculins as shared with other toxins mainly consists of three loops forming a large and flat triple-stranded antiparallel β-sheet (Kinemage 1; le Du et al., 1992; Pillet et al., 1993). In Fas1 the β-sheet is formed by residues Cys 22–Arg 27, Val 34–Cys 39, and Leu 48–Cys 53. Formally Cys 3–Cys 4 and Leu 14–Thr 15 also form a β-strand. Loop I consists of residues 5–15, loop II of residues 24–38 and loop III of residues 43–50 (le Du et al., 1992).

Fasciculin 1. The vast majority of residues of Fas1 are solvent accessible. Only two, the disulfide-linked Cys 3 and Cys 22, show no solvent accessibility. Several residues (Tyr 4, Leu 14, Tyr 23, Arg 37, Leu 48) are only partly solvent accessible. Several of these residues located in homologous positions on other toxins are less accessible. Virtually all potentially charged residues in this family of toxins are fully accessible to solvent; only Arg 37 is partly accessible.

Initial observations of the three-dimensional structure of Fas1 reveal the following distribution of charged residues (Kinemage 1). The electrostatic fields produced by the cationic side chains of Arg 11, Lys 25, Arg 27, and the anionic side chains of Asp 45 and Asp 46 are located on a common surface area of the molecule. This confers a small overall positive charge to this side. The cationic side chains of Arg 24, Arg 37, Lys 51, Lys 58, the obliquely oriented side chains of Arg 28 and Lys 32, and the negatively charged side chains of Asp 57, Glu 49, and carboxyl-terminus of Tyr 61 are located on the opposite surface of the molecule. Cationic residues Arg 27, Arg 28, and Lys 32 are located at the tip of loop II, whereas anionic Glu 19 and positive amino-terminus of Thr 1 reside on the opposite end of the molecule.

There are three significant clusters of hydrophobic residues in this molecule: (1) a cluster that contains Pro 42, Pro 43, and Val 50 of loop III and Tyr 23 of loop II; (2) a cluster that contains Leu 48 and Tyr 47 of loop III, the hydrophobic portion of the side chains of Arg 27, and Leu 35 of loop II; (3) a cluster formed by Tyr 4 and Leu 14 of loop I, and the hydrophobic parts of the side chains of Lys 58 and Tyr 61 located in the area of the disulfide core of the molecule. This system of hydrophobic clusters likely stabilizes the overall structure of the fasciculin molecule, as found for other toxins (Fig. 1B).

Salt bridges formed between positively charged residues of loop II and negatively charged residues of loop III constrain these loops significantly in Fas1; such strong electrostatic constraints do not occur in the α-neurotoxins, Ebt, Bgt, α-cobratoxin (Cbt), and in cardiotoxin V_4^{II} (Cdt). Those bridges impart additional rigidity to the fasciculin molecule loops when compared with the homologous α-neurotoxins.

Fasciculin 2. Fas1 and Fas2 differ by single substitution Tyr 47 Asn. This difference does not affect the rigidity of the fasciculin molecule because all of the strong electrostatic constraints between loop II and loop III are maintained in the presence of the Asn residue (Fig. 1C).

Fasciculin 3. In Fas3 two additional charges appear in loop I: Lys 15 and Asp 16 (Fig. 1D). These are significant modifications because Arg 11 is the lone positive charge in this area for Fas1 and Fas2. In the minimized structure of Fas3 Lys 15 is not linked by any salt bridge to other residues. This imparts an additional density of positive charges in the loop I area. The negative charge on Asp 16 is mostly compensated by the amino-terminus strengthening rigidity of loop I together with an additional (Ile 2–Leu 14) hydrophobic interaction. Because Fas3 has an order of magnitude higher affinity than Fas1 for rat brain AChE (Marchot et al., 1993), this positively charged area of loop I is presumed to contribute substantially to the stabilization energy for Fas3 binding to AChE.

Structural bases of functional properties

To determine the structural features in the fasciculin molecule that contribute to its mode of action, we compared the three-dimensional structures of the fasciculins to those of α-neurotoxins, which are antagonists at the nicotinic receptor: Cbt, Bgt, Ebt (Fig. 1B), and to that of Cdt. Fas1 shows substantive differences at the following positions.

Loop I. Conservation of Arg 11 is a feature unique to the fasciculins. Only four α-neurotoxins out of a family of 104 have a positively charged residue in this position, but two of them have a neighboring negative residue yielding charge compensation (Endo & Tamiya, 1987). Several α-neurotoxins (19 out of 104) have a negatively charged residue in this position. The maps of toxins shown in Figure 1 reveal the uniqueness of Arg 11, contributing to the exposed positive charge of its loop I to the electrostatic profile of fasciculin. Similar positive residues are not found in Bgt and Ebt (Fig. 1B). The uncompensated positively charged residue Lys 15 of Bgt and Ebt is located much closer to the base of loop I and to the amino-terminal positive residue Thr 1. Accordingly, it does not change significantly the electrostatic profile in the area of the amino-terminal residues. Lys is the most common residue for α-neurotoxins in position 15. A far smaller number of α-neurotoxins (12 of 104) have a positively

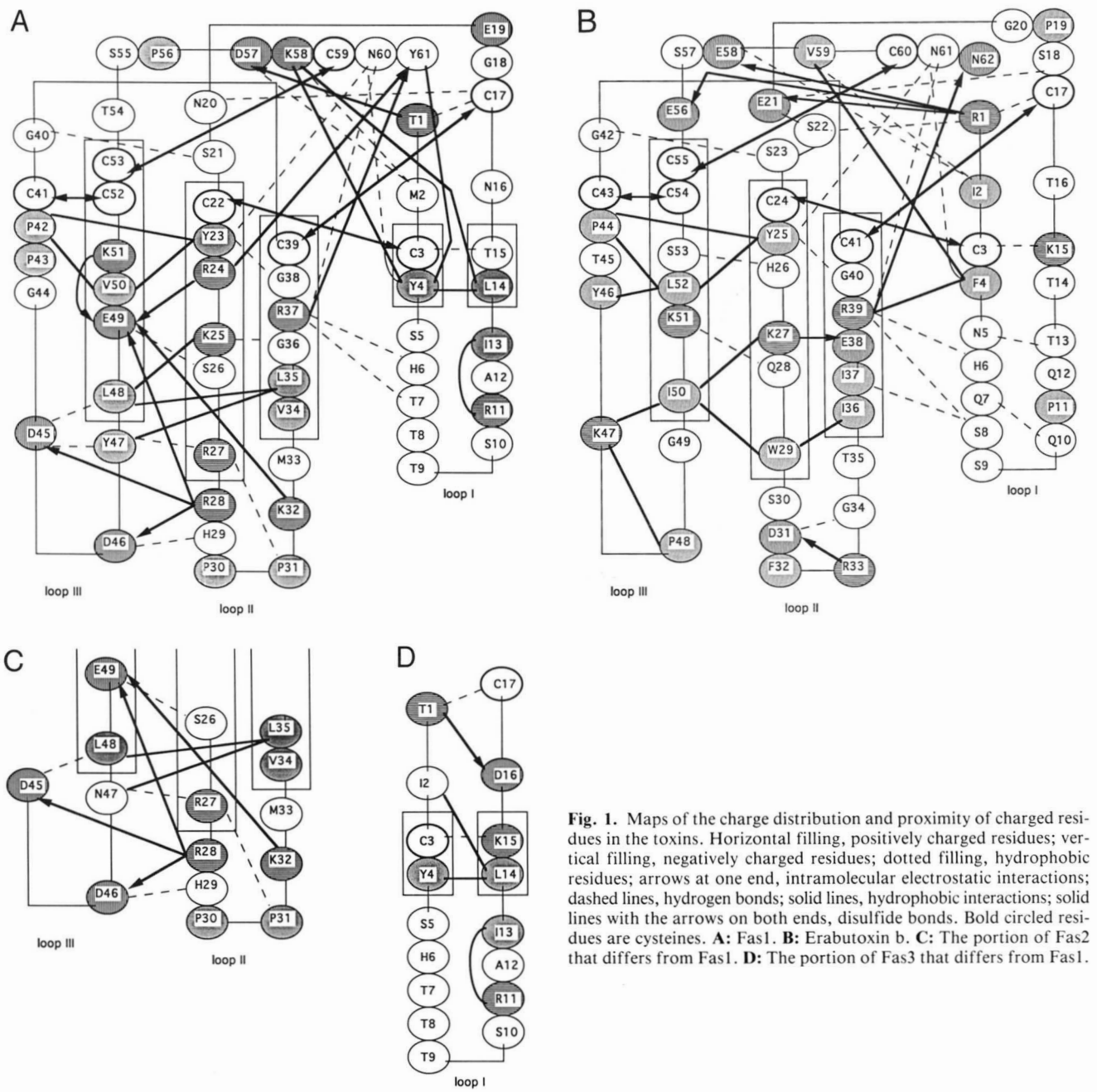

Fig. 1. Maps of the charge distribution and proximity of charged residues in the toxins. Horizontal filling, positively charged residues; vertical filling, negatively charged residues; dotted filling, hydrophobic residues; arrows at one end, intramolecular electrostatic interactions; dashed lines, hydrogen bonds; solid lines, hydrophobic interactions; solid lines with the arrows on both ends, disulfide bonds. Bold circled residues are cysteines. **A:** Fas1. **B:** Erabutoxin b. **C:** The portion of Fas2 that differs from Fas1. **D:** The portion of Fas3 that differs from Fas1.

charged residue in position 13. In Cbt, the positively charged Lys 12 is compensated by negative Asp 13, and the electrostatic field only influences the very amino-terminal residues Ile 1 and Arg 2. These differences cause significant changes in electrostatic field distribution between the fasciculins and the α-neurotoxins (Fig. 2). The specific positioning of positive residues Lys 12 and Lys 5 in Cdt differs from Cbt, Ebt, and Bgt, and confers to loop I an electrostatic profile closer to that of fasciculin.

Loop II. The noteworthy feature of loop II in the fasciculin molecule is the presence of six positively charged residues: Arg 24, Lys 25, Arg 27, Arg 28, Lys 32, and Arg 37. Two of them, Lys 25 and Arg 27, are weakly compensated. Nevertheless, these residues are positioned to have the nearest opposite charge neighbor at the distance about 8 Å. The closest negatively charged residue to Arg 11 is more than 21 Å away. In this arrangement the charge on Arg 11 is more likely to interact with a distant charge on AChE than would the charges on Lys 25 and Arg 27. The difference between energies of interaction with AChE of the uncompensated charge and dipole are significant at the distance of 20 Å. These considerations point to an uncompensated charge of Arg 11 from loop I playing the more significant role in fasciculin docking to the surface of AChE. Other toxins have much smaller differences in charges between loops. In Ebt (Figs. 1B, 2B) the charges of polar residues are compensated, creating pairs of opposite charged residues within the

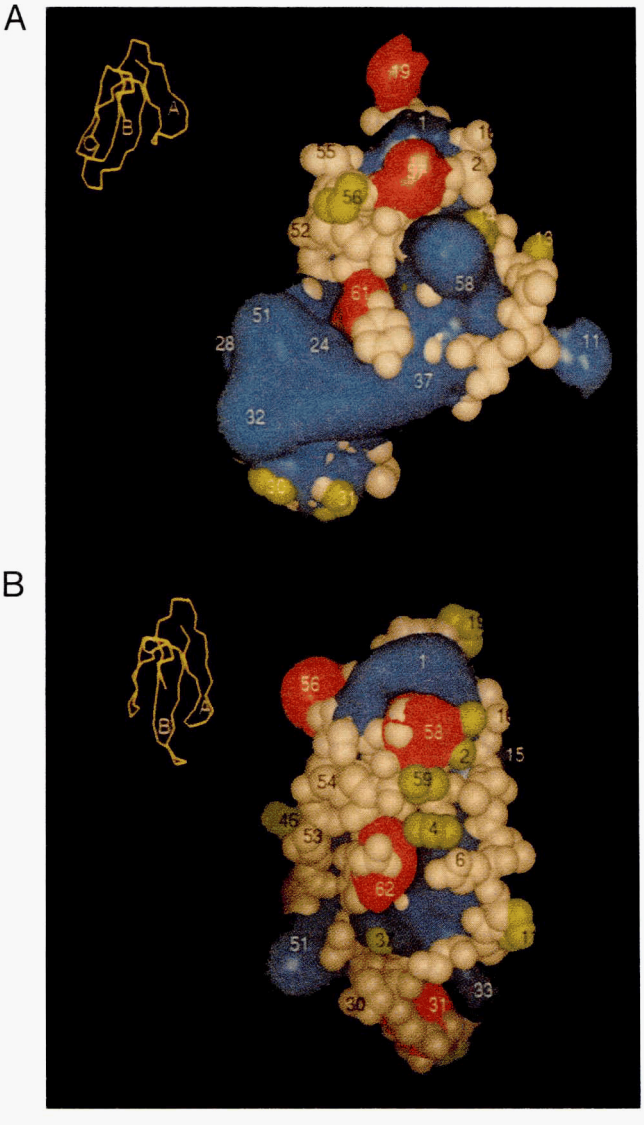

Fig. 2. Electrostatic isopotential surfaces superimposed with the CPK model (gray spheres) of toxins. The red surface corresponds to the isopotential contour $-1\ kT/e$, and the blue surface corresponds to the isopotential contour $+1\ kT/e$, where k is the Boltzmann constant, T is temperature, and e is the electronic charge. In the upper right quadrant is shown the α-carbon structure oriented with the CPK model. **A:** Fasciculin 1. **B:** Erabutoxin b.

loop: Asp 31–Arg 33, Lys 27–Glu 38. The residue Arg 39 is partly compensated by the carboxyl-terminal charge, and as a result, the overall charge of this loop in Ebt is smaller. A similar situation exists in Bgt where compensating pairs are created: Asp 30–Arg 36 and Arg 25–Glu 56, whereas Glu 41 and Lys 26 are not close enough for charge compensation. The overall positive charge of loop II is mainly due to uncompensated Lys 38. In Cbt, loop II contains four cationic residues and two anionic residues, which makes its overall charge positive. Cdt has a distribution of positive charges close to fasciculin, but the position of uncompensated cationic residues, Lys 29 and Lys 30, at the tip of loop II makes it possible for this loop to play a significant role in the binding of this toxin.

Some of the positive charges in loop II are not specific to fasciculin: Arg 24 (represented by Arg 25 in α-Bgt and by Lys 23 in Cdt) and Lys 25 (represented by Lys 26 in α-Bgt and by Lys 27 in Ebt). The short neurotoxins of 60–62 amino acids (Karlsson, 1984; Endo & Tamiya, 1987) often have both of these positive charges on positions 24 and 25. For Ebt, Lys 27 was proposed to be at the receptor binding site (Faure et al., 1983; Martin et al., 1983; Pillet et al., 1993). Arg 37 is common to many toxins represented as Arg 39 in Ebt and Arg 36 in Cdt (Rees et al., 1990). However, the following residues are unique to the fasciculins:

Arg 27: The majority of short α-neurotoxins, Ebt (residue 29), Cbt (residue 25), and long neurotoxin α-Bgt (residue 28) have a Trp residue at this position. Trp is conserved as a part of a β-strand and is also thought to be involved in the binding of the these toxins to the nicotinic receptor (Faure et al., 1983; Pillet et al., 1993).

Arg 28: Although present in 23 of 104 three-fingered toxins (Endo & Tamiya, 1987), this positive charge in all fasciculins is immediately compensated by the highly conserved neighboring residue, Asp 46 from loop III.

Phe 31 in fasciculins is substituted in many α-neurotoxins for a positively charged residue (Arg 33 in Ebt, Arg 33 in Cbt, Lys 30 in Cdt). A possible role for this residue in α-neurotoxins is to create a specific electrostatic profile selective for the nicotinic acetylcholine receptor (nAChR) binding site.

Lys 32 is present only in fasciculins. Although no other toxin has a positive charge in this position, many contain a positive residue at position 33 or 34.

Loop III. This loop in the fasciculins has unique characteristics due to two negatively charged neighbors Asp 45 and Asp 46. Instead of Asp 45 most α-neurotoxins have a positive charge in the corresponding position (Lys 49 in Cbt, Lys 47 in Ebt, Lys 52 in Bgt). Only 9 of 106 members of the three-fingered toxin group have a negatively charged residue in this area. Only the fasciculins have a negative charge at position 46. Also, no short α-neurotoxin has a negative charge in position 49 (Glu 49 in Fas), although about 30% of long α-neurotoxins have negatively charged residues close to this position (Asp 53 in Cbt, Glu 56 in α-Bgt).

Lys 51 appears less important to specificity. About 5 three-fingered toxins have the negatively charged group in the closest position (equivalent to 51 in Fas), whereas 30 of 104 toxins have a positively charged residue in this position (Endo & Tamiya, 1987).

Precollision orientations of Fas1 and AChE

The most favorable electrostatic energies of intermolecular interaction for almost all rotational orientations of Fas1 (lowest in the free energy profile) are found in the sectors of orbits (Fig. 3): circles 1, 2, and 5 from $-45°$ to $45°$; circles 3 and 4 from $0°$ to $90°$. This first step of selection gave a significant reduction in the number of possible bound conformations of Fas1.

Rotational conformers that minimize electrostatic energy were selected more precisely in the next step. The highest energy levels occur when charges of the same sign come in close apposition to each other, and the lowest occur when these charges are distant and the opposite charges are proximal. Table 1 shows the most favorable rotational positions of Fas1 in a precollision

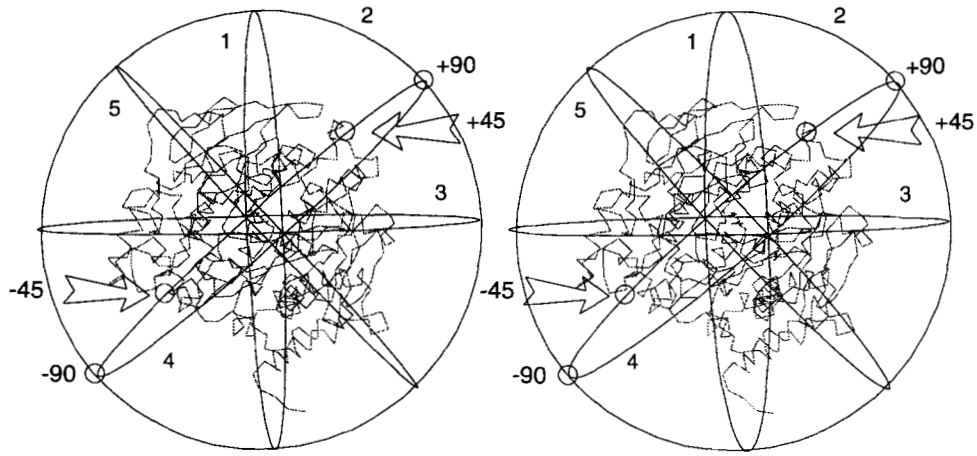

Fig. 3. Stereo view of five circular tracks along which the Fas1 molecule was moved across the acetylcholinesterase surface for evaluating intermolecular electrostatic energy. Shown is the AChE orientation with a central axis perpendicular to the plane of the paper, entering the active center gorge.

orientation to AChE. The main low-energy positions are *X*, *Z* and *Y*, *X*, which occur in all circles. We also included other low energy positions for further investigation: *Y*, $-Z$; *Y*, $-X$; *Z*, $-Y$; $-Y$, *Z*. The chosen positions (Table 1) were further investigated with the addition of five rotational Fas positions to increase the overall number of investigated positions to 15. To avoid overlooking of possible positions generally due to the digital increments of angles, only the very high energy positions were eliminated. The selected positions were investigated with 6° increments of orbital rotation.

In each orbital position, three orientations with the lowest energy were chosen. These energy values are shown in Figure 4. Regions where the electrostatic energy values are the most favorable were selected at each orbital circle. The selected positions are: circle 1: angles from −30° to 6° and angles from 12° to 36°, orientations *X*, $-Y$ and *X*, *Z*; circle 3: angles from −48° to −30°, orientations *X*, $-Y$ and $-Y$, *X*; angles from 36° to 54°, orientation *X*, $-Y$; *X*, $-Z$ and *X*, *Z*; circle 4: angles from −24° to 6°, orientations *X*, $-Y$ and *X*, $-Z$; angles from 24° to 42°, orientations *Y*, *X* and *X*, *Z*; circle 5: angles from −42° to −18°, orientations *X*, *Z* and *X*, *Z*.

The area of the most favorable AChE-Fas1 interactions is shown on Figure 5A. This specific area surrounds the gorge entrance of AChE. By investigating the precollision orientation of Fas1, the results were refined. The preferred orientation of Fas is found to vary with its translational position. At the central point (Fig. 5A) position *X*, *Z* is favored, as the loops of Fas1 are directed toward the entrance of the gorge. Around the central point (0°), the *X*, *Z* orientations are preferred to $-X$, *Z* for all circles. In the *X*, *Z* orientation the electrostatic field direction of Fas1 roughly points toward the enzyme. The large negative electrostatic potential existing in this region of AChE (Ripoll et al., 1993; Tan et al., 1993) is the basis for the favorable interactions with the positively charged loops I and II of the fasciculin molecule.

Loop I is more likely to be oriented toward the enzyme than loop III because on one hand *Y*, *X*; *X*, $-Z$, and *X*, $-Y$ rotations have very low energies and on the other hand $-X$, $-Z$ and *Y*, $-X$ rotations have very high values. It appears that loop I is attracted toward the right side of AChE defined by an angle of 90° in circle 3 (Figs. 3, 5A). When the Fas1 molecule is moved on circle 1 from −30° to 30°, the most preferred orientation is changed from *X*, $-Y$ to *X*, *Z*, again turning loop I toward the right side of the AChE molecule (Fig. 3).

Orientation *X*, $-Y$ with the loop tips toward the right side of the gorge (Fig. 3) is more favorable than $-Z$, $-X$. Movement toward this side is nearly parallel with the general direction of the electric field in the AChE molecule.

Analyses of the preferred orientations of all circles over a 10-Å intermolecular distance reveal that the electric fields of AChE

Table 1. *Favorable orientations of Fas1 as found at the various circles (according to Fig. 3)*

Circle	−45°	0°	+45°	90°
1	*Y*, *X*	*X*, *Z*; *Y*, *X*	*X*, *Z*; *Y*, *X*; *Z*, $-Y$	
2	*Y*, $-Z$	*X*, *Z*; *Y*, *X*; *Z*, $-Y$	*X*, *Z*	
3		*X*, *Z*	*X*, *Z*; *Z*, $-Y$	*X*, *Z*; *Y*, *X*
4		*X*, *Z*; *Y*, *X*	*X*, *Z*; *Y*, *X*; *Z*, $-Y$	*X*, *Z*; *Y*, *X*
5	*Y*, *X*; *Y*, $-X$; *Z*, $-Y$	*X*, *Z*; $-Y$, *Z*	*X*, *Z*	

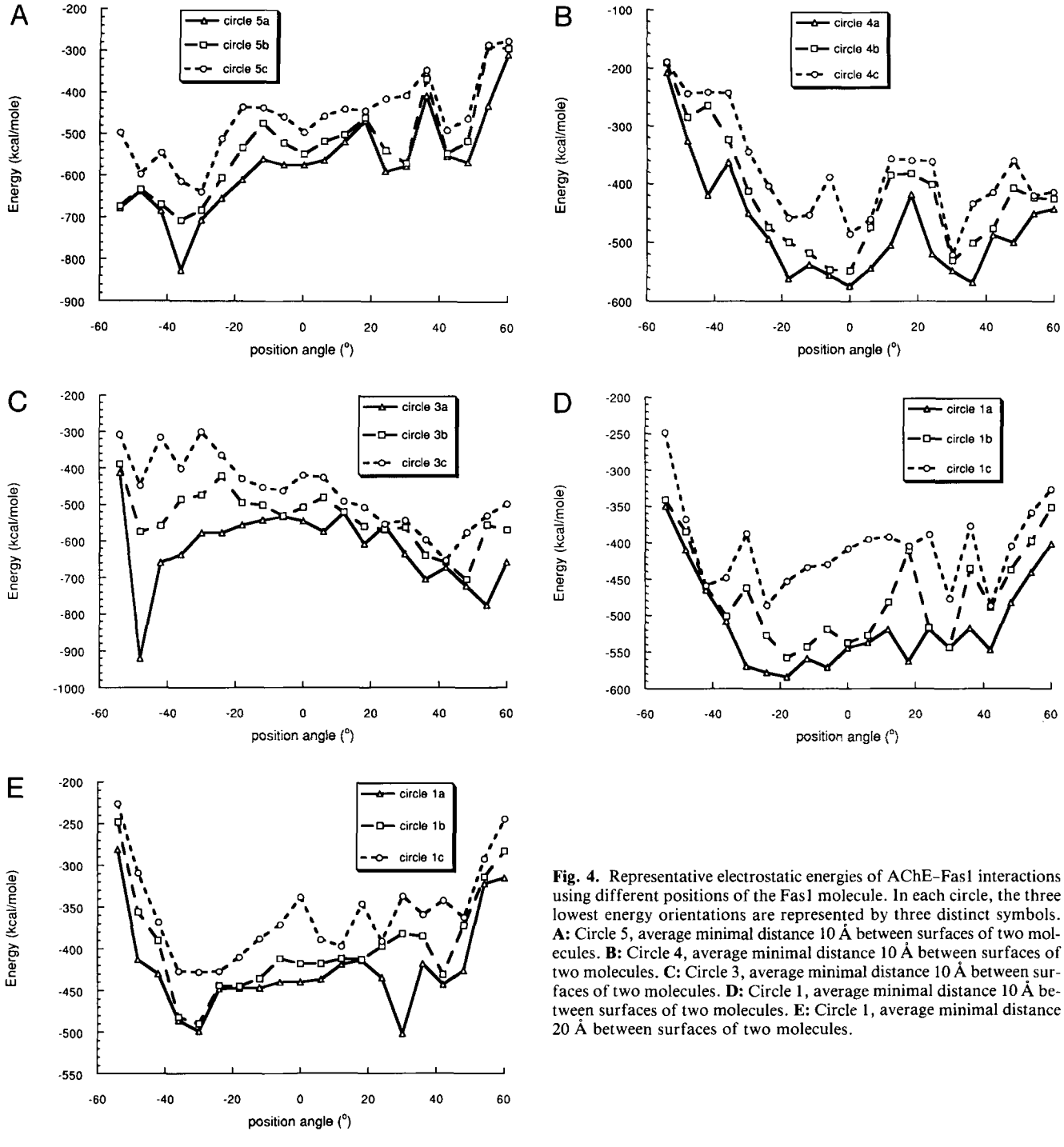

Fig. 4. Representative electrostatic energies of AChE-Fas1 interactions using different positions of the Fas1 molecule. In each circle, the three lowest energy orientations are represented by three distinct symbols. **A:** Circle 5, average minimal distance 10 Å between surfaces of two molecules. **B:** Circle 4, average minimal distance 10 Å between surfaces of two molecules. **C:** Circle 3, average minimal distance 10 Å between surfaces of two molecules. **D:** Circle 1, average minimal distance 10 Å between surfaces of two molecules. **E:** Circle 1, average minimal distance 20 Å between surfaces of two molecules.

and Fas1 are closely aligned. This suggests an approach with either Arg 11 of loop I or the tip of loop II facing toward the gorge of AChE. At intermolecular distances greater than 15 Å, the differences between various orientations of Fas1 begin to vanish.

Hence, a focused electrostatic guidance of Fas1 alone leads to a precollision position at the surface of the AChE molecule, near the gorge entry. This position results mainly from the orientation of the electrostatic fields of AChE and Fas1. The next step is the determination of possible AChE-Fas1 complexes.

Complexation of AChE and Fas1

The orientations of Fas1 with loop I and the tip of loop II approaching the region of the aromatic triad cluster (Tyr 70, Tyr 121, Trp 279) at the peripheral site of AChE were considered for further analysis. These three residues residing at the rim of the AChE gorge account for the selectivity of the fasciculins for AChE over BuChE (K_I = 2 pM versus 200 μM for mouse enzymes) (Radić et al., 1994). The distance between Arg 11 of

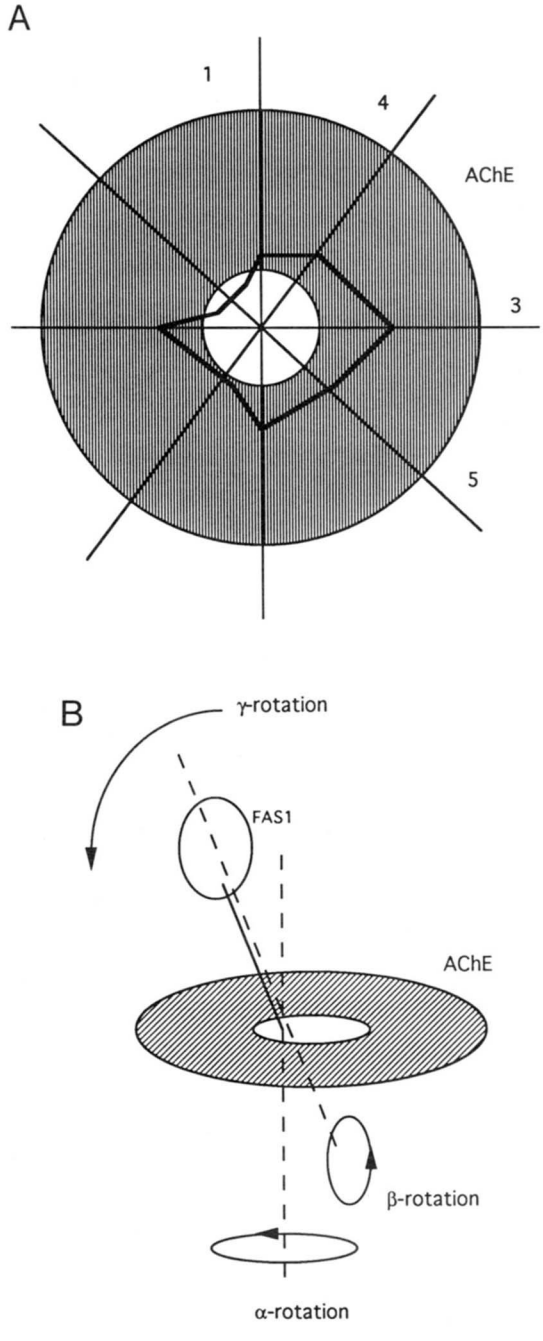

Fig. 5. Interaction of Fas1 with recognition site on AChE. **A:** Area of possible binding of Fas1 on the surface of AChE calculated from the precollision orientations (lighter area is the simplified region of the gorge). Position of the AChE peptide chain is shown in Figure 3. **B:** Movement of the Fas1 molecule during the complexation procedure.

Fas1 and each amino acid of the AChE peripheral aromatic triad cluster was constrained to 4–6 Å. Putative complexes were formed in two steps. Firstly the Fas1 molecule was rotated along its *y*-axes (Fig. 5B) for a complete circle of 360° in 30° increments (α-rotation). At each 30° position, Fas1 was rotated along its β-axis in 30° increments again in a complete circle. The β-axis starts at the center of the peripheral aromatic triad cluster and leads to the center of Fas1. Then, after each Fas1 β-rotation, an AChE–Fas1 complex was created by moving the Fas1 molecule (γ-rotation) toward AChE surface to maximize intermolecular contacts within the distance where van der Waals forces could be considered. The three rotations are depicted in Figure 5B. In this way, 144 putative complexes were generated.

The orientations of AChE and Fas1 side chains in selected complexes were then minimized to make the complex less dependent on the fixed orientations of the respective crystal structures. Sixty complexes of lowest interaction energy were selected. After minimization the final energy values showed a significant drop and were nearly equivalent. About 90% of this energy arises from the electrostatic component and the remainder from van der Waals' forces. A similar general pattern of local minimal energies was seen for both cutoff distances of 12 Å and 100 Å. We eliminated the largest electrostatic energy complexes. Forty-one complexes remained after this selection. The following selection was based on the electrostatic energy and buried surface calculations. For the selected complexes the range of electrostatic energies at a 100-Å cutoff distance were from −663 to −1,014 kcal/mol; at a 12-Å cutoff distance, they were from −439 to −807 kcal/mol and the buried surface areas ranged from 832 to 2,378 $Å^2$. The absolute values of energies do not have a specific reference point, and we considered only the differences between these energies for various complexes. The electrostatic energy values with the 12-Å cutoff mainly reflect the short-range interactions of fasciculin with AChE and 100-Å cutoff values also encompass the long-range electrostatic interactions. Taking into account the numerous approximations of theoretical calculations of this kind, we used both energy values for the selection of complexes. For six selected complexes, the values of these parameters are the following: complex 25: electrostatic energy (100 Å) −1,015 kcal/mol, electrostatic energy (12 Å) −767 kcal/mol, buried surface 1,688 $Å^2$; complex 36: −927 kcal/mol, −734 kcal/mol, 1,431 $Å^2$; complex 39: −860 kcal/mol, −808 kcal/mol, 1,508 $Å^2$; complex 45: −823 kcal/mol, −698 kcal/mol, 1,411 $Å^2$; complex 58: −862 kcal/mol, −699 kcal/mol, 1,216 $Å^2$; complex 60: −880 kcal/mol, −697 kcal/mol, 1,300 $Å^2$. Other complexes with larger buried surface areas have the higher electrostatic energy values and were eliminated. Complex 25 appears most favorable among the list, where it is found to have the global minimum of electrostatic energy (100 Å) and close to the global minimum in 12-Å cutoff calculations. It also has a substantial buried surface area.

We then calculated the favorable interactions between side chains of fasciculin and AChE of these complexes to make a final selection. We find that complex 36 has the same intermolecular interactions as complex 25 and very similar energy values. It falls into the same family as complex 25 and was eliminated because of slightly higher energy than complex 25. Similarly, two complexes, 45 and 39, happen to be in one family, and complex 39 was chosen. Complexes 58 and 60 were also nearly identical, but complex 58 has the larger number of favorable intermolecular contacts (Table 2), so it was selected.

Three complexes emerged based on optimizing the parameters used in this strategy: 25, 39, and 58. Table 2 shows the residues of AChE in contact with Fas1 in the selected complexes. Table 3 shows their intermolecular interactions, and the coordinates of the complexes are contained in the Electronic Appendix. A comparison of possible contacts of AChE and BuChE in the final complexes leads to the following considerations.

Table 2. *Calculated contact regions of the AChE-Fas1 complexes*

Complex	Contact residues of *Torpedo* AChE
25	70-76, 121, 279-280, 285-287, 332-342, 348-358, 362-372
39	68-78, 120-121, 250-256, 265-285, 333-336
58	39-42, 63-93, 121, 268-285, 333-336

Complex 25 (Fig. 6A; Kinemage 2)

In this complex, Arg 24, Arg 27, and Arg 28 in Fas1 are likely to be stabilized by negative charges in AChE, of which Glu 350 is a primary candidate. Because this residue exists as Lys in BuChE, the change in binding energy associated with the mutation would be one means for assessing this complex.

Complex 39 (Fig. 6B; Kinemage 3)

Near the contact positions in this complex, several residue differences exist between AChE and BuChE: Glu 73 Gln, Glu 268 Asn, Lys 270 Asp, Asp 276 Leu, and Asp 285 Gly. Some of these substitutions might be expected to diminish the contributions of Arg 11 and Arg 37 in Fas1 for stabilization of this complex. Substitution of Glu 268 Asn in the AChE molecule should result in the loss of the Arg 27-Glu 268 interaction. Substitution of Lys 270 Asp should result in the loss of the Asp 45-Lys 270 interaction and create repulsion between two negatively charged side chains. Substitution of Asp 276 Leu should result in loss of interaction with Arg 24, Lys 25, and Arg 37. Substitution of Asp 285 Gly should diminish the attraction of Arg 11 toward the gorge.

Complex 58 (Fig. 6C; Kinemage 4)

The area of intermolecular interactions in this complex is nearly identical for AChE and BuChE and points to the aromatic triad cluster (Tyr 70, Tyr 121, Trp 279) at the peripheral site as primarily accounting for the selectivity differences between AChE and BuChE.

Discussion

Taking into consideration the high electrostatic potential of AChE and its unique surface charge distribution oriented toward the gorge, one may assume that these factors can play a decisive role in guidance of the molecules found to associate with AChE. Recent theoretical calculations revealed the importance of this concept for association of cationic substrates with AChE (Ripoll et al., 1993; Tan et al., 1993). The question of specificity of peptide toxin binding to AChE is critical because among the family of more than 100 three-fingered toxins, only the fasciculins bind with high affinity to AChE.

Elimination of surface charges peripheral to the gorge through mutagenesis appeared to have little influence on substrate catalysis (Shafferman et al., 1994). However, several changes within the gorge itself were not included in the permutations of mutations. Glu 199 and Glu 443 within the gorge are critical for both inhibitor binding and catalysis (Radić et al., 1992, and unpubl. data). Other anionic residues also exist within or near the gorge, which give rise to mutant enzymes with sufficiently low

Table 3. *Contact residues of Fas1 (shown in italics) and Torpedo AChE in the selected complexes*

	Electrostatic interactions		Hydrophobic contacts		
Complex	<6 Å	6-9 Å	<4 Å	4-5 Å	Possible hydrogen bonds
25	*R24*-E350 *R24*-D351 *R27*-D365 *R27*-D369 *R37*-D351 *K51*-E350	*R11*-D72 *R11*-D276 *K32*-E350 *R37*-D285 *R37*-E350	*P31*-L368 *L35*-K357 *R37*-P337	*R27*-L368 *P31*-V356 *Y61*-P337	*T7*-D285 *T9*-P337 *T9*-G338 *S10*-L332 *R11*-Y70 *R11*-W279 *R24*-E350 *R27*-V365 *K32*-M353 *Y61*-D351
39	*R11*-D72 *R27*-E268 *R27*-E273 *D45*-K270	*R24*-E273 *R24*-D276 *K25*-D276 *R37*-D276 *D46*-K270	*P31*-K269 *L35*-K270 *Y47*-K270 *L48*-K270	*I13*-P76	*S5*-E73 *H6*-Y70 *R11*-Y70 *R11*-Y334 *Y47*-E268
58	*R11*-D72 *R27*-E89 *R37*-D276	*D45*-R88 *K25*-E73 *K25*-E82 *R24*-D276 *R27*-E89 *R27*-E92 *R27*-D93 *R37*-E73	*P31*-P271	*P31*-K270	*H6*-Q74 *H6*-Y70 *T7*-V71 *S10*-D276 *R11*-Y70 *R37*-E73 *Y47*-E89

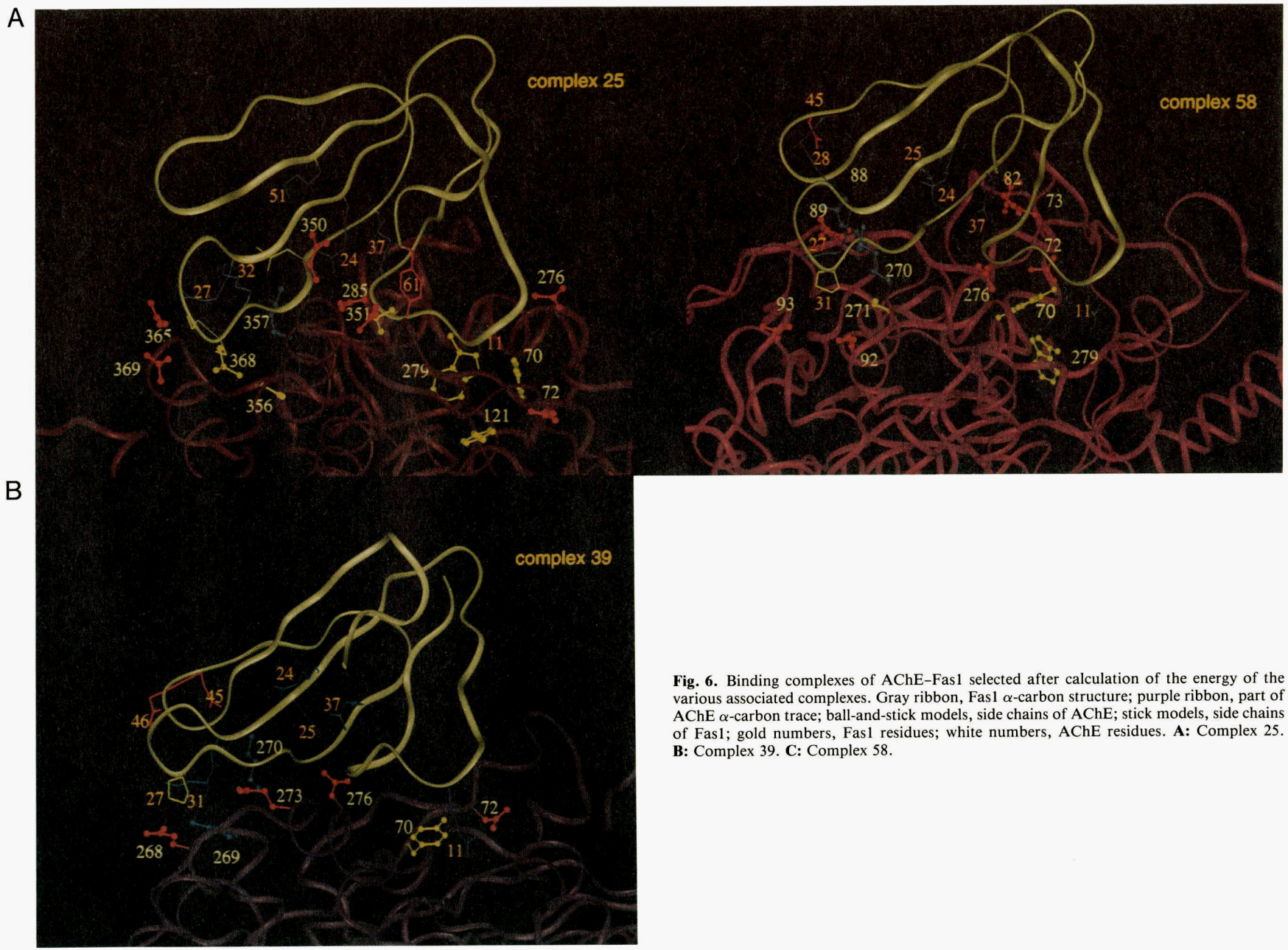

Fig. 6. Binding complexes of AChE–Fas1 selected after calculation of the energy of the various associated complexes. Gray ribbon, Fas1 α-carbon structure; purple ribbon, part of AChE α-carbon trace; ball-and-stick models, side chains of AChE; stick models, side chains of Fas1; gold numbers, Fas1 residues; white numbers, AChE residues. **A:** Complex 25. **B:** Complex 39. **C:** Complex 58.

activity to preclude study. This may point to a cluster of charges focused toward the gorge as being responsible for the associations of small ligands and the orientation of associating fasciculin.

The potential intramolecular interactions stabilizing loop III in Fas1 relative to Fas2 can be compared to the increase in number of interactions in loop I of Fas3 relative to Fas1 and Fas2. Only Fas3 has an appreciably higher affinity among the fasciculins (Marchot et al., 1993), which suggests that loop I could play the more important role in association of Fas and AChE. The six positively charged residues in loop II of fasciculin with their distinctive charge compensation are likely to be critical for its orientation toward the enzyme. These differences create an electrostatic potential for Fas unique among the three-fingered toxins. Our calculations of precollision orientation of Fas1, which took into account only the charge distribution on AChE and Fas1 and no other preconditions, resulted in positioning of the fasciculin molecule in the region of AChE close to the gorge entrance and near the three aromatic residues that have been shown by mutagenesis to be involved in the AChE–fasciculin interaction (Radić et al., 1994). Electrostatic guidance calculations can therefore lead to a reasonable positioning of fasciculin in apposition to a specific region of AChE. The drastic change of electrostatic field of AChE after the binding of Fas (Fig. 7) can definitely affect the electrostatic guidance mechanism of the AChE–fasciculin complex toward subsequent entry of charged substrates. Recent kinetic experiments where fasciculin can serve as an allosteric activator and/or inhibitor of AChE depending on the nature of the substrate and mutated residues (Z. Radić

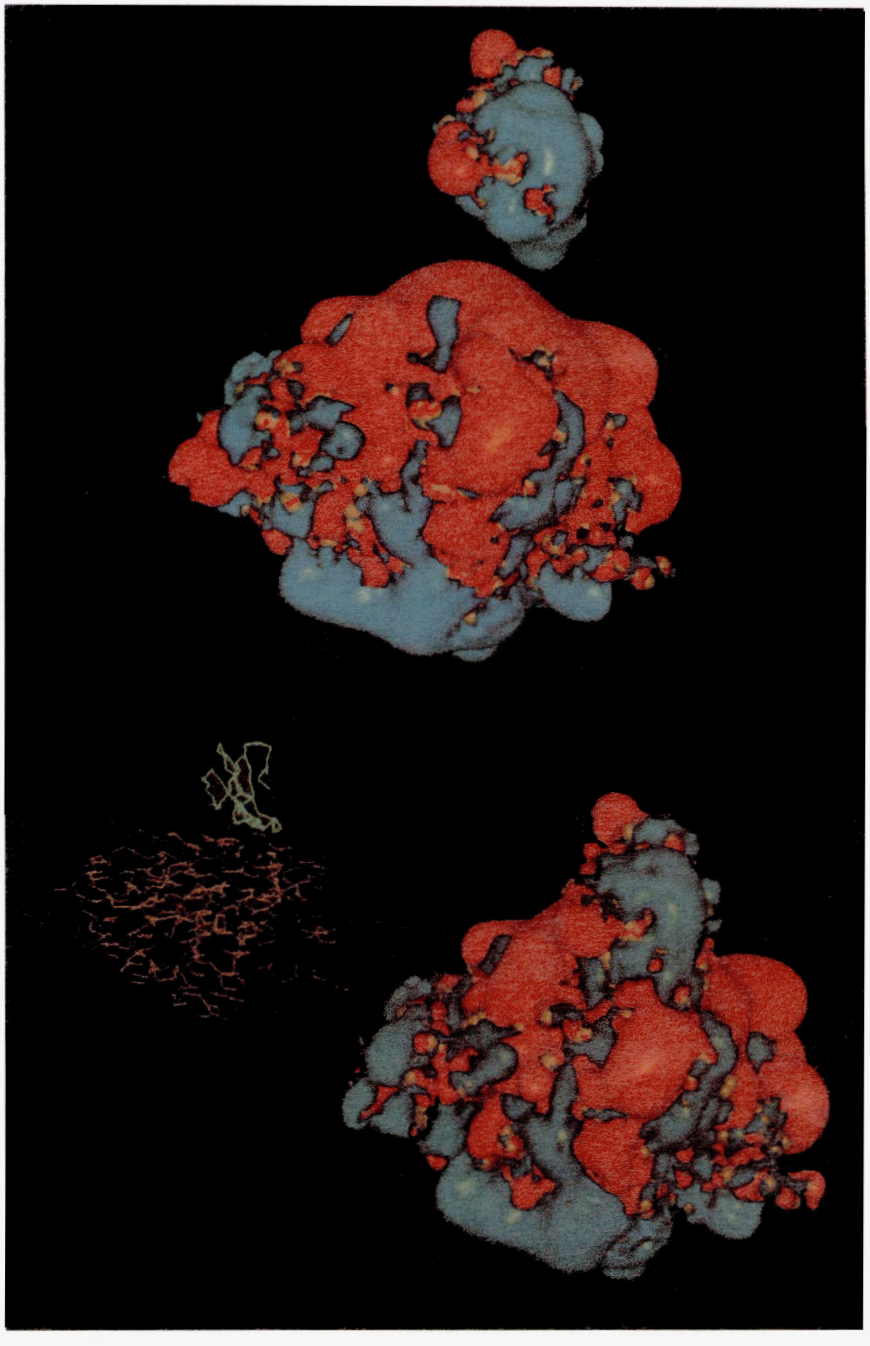

Fig. 7. Electrostatic isopotential surfaces of Fas1 and AChE. Orientation of the proteins is the same in A and B. Red surface corresponds to the isopotential contour $-1\ kT/e$; blue surface corresponds to the isopotential contour $+1\ kT/e$. **A:** Free state. **B:** Bound state of the complex.

D. Quinn, D. Vellom, S. Camp, & P. Taylor, submitted for publication) are in accord with this notion. Calculations of the buried surface of the complex delimited the possible orientations of the complex to a number realistic for designing mutagenesis studies on fasciculin and AChE.

Of the three complexes (Fig. 6A,B,C), for complexes 58 and 39, Fas is located on the surface of AChE, actually capping a disulfide loop between residues Cys 60 and Cys 97. This loop serves as a flap that opens the binding site for substrates in *Candida rugosa* and *Rhizomucor miehei* lipases (Brzozowski et al., 1991; Grochulski et al., 1994). These enzymes show homology in sequence and overall α-β-hydrolase fold characteristics of AChE (Ollis et al., 1992). Hence, it is possible that the diminished catalytic capacity of the fasciculin–AChE complex may also arise from constraints imposed on this region that restrict the conformational flexibility of AChE.

The known three-dimensional structures of Fas1 (le Du et al., 1992) and AChE (Sussman et al., 1991) allow for multiple and complementary approaches to study the complex. Initial studies showing competition between propidium and fasciculin pointed to fasciculin interactions not occurring at the active center of the enzyme (Karlsson et al., 1984). Subsequent studies showing that fasciculin will bind to the DFP-conjugated enzyme and that the active center of AChE can be phosphorylated by DFP when fasciculin is bound (Marchot et al., 1993) provide important documentation of accessibility to the active center gorge in the complex. Site-specific mutagenesis has revealed that residues that form the acyl pocket and the choline binding site have minimal influence on fasciculin binding, whereas modification of three residues Trp 279, Tyr 121, Tyr 70 at the rim of the gorge have the major influence and can actually account for the free energy difference of fasciculin binding to AChE versus BuChE (Radić et al., 1994). Moreover, the importance of cation–π-electron interactions that could arise between positively charged residues of fasciculin and this aromatic cluster have been well documented in quantum chemical calculations (Kim et al., 1994). Hence, the surface for binding can, at least in part, be defined by this aromatic cluster at the top of the gorge.

At present, there is only fragmentary chemical modification data and no mutagenesis evidence with the fasciculin molecule to aid in assignment of interacting residues. Cervenansky and colleagues (1994) have shown that acetylation of residues Lys 25, Lys 32, and Lys 51 of Fas2 partly reduces its interactions with AChE. These three residues appear involved in the intermolecular stabilization of loop II in fasciculin and their modification may lead to destabilization of its rigid structure, a finding not revealed upon examination of the CD spectra of the modified molecule. Also, in our calculations Lys 51 and Lys 32 are shown to play a role in electrostatic interactions with AChE in complex 25. Lys 25 is involved in electrostatic interaction with AChE in complexes 39 and 58 (Table 3). The theoretical considerations presented here define the unique features of the fasciculin structure and should enable us to distinguish the more probable binding orientations of the complex.

Methods

Initial protein structures

The crystallographic coordinates of *Torpedo* AChE, code 1ACE (Sussman et al., 1991), Fas1, code 1FAS (le Du et al., 1992), α-bungarotoxin, code 2ABX (Bgt) (Love & Stroud, 1986), cardiotoxin V_4^{II}, code 1CDT (Cdt) (Rees et al., 1990), erabutoxin b, code 3EBX (Ebt) (Smith et al., 1988), and α-cobratoxin, code 1CTX (Cbt) (Walkinshaw et al., 1980), were retrieved from Brookhaven Protein Data Bank (WWW: http://www.pdb.bnl). All structures were reexamined to add unresolved atoms with Insight 2.3.0 and Homology programs (Biosym Technologies, Inc., 1994, San Diego, California). Charges were assigned according to average pK_a's of the ionizable side chains at pH 7.5. We performed the short steepest decend minimization cycle to relieve strain in the side chains and also energy minimized the regions that deviated from the crystal structure with the Discover program (Biosym Technologies, Inc., 1994). Raman and NMR spectroscopy show general agreement between the solution and crystal structures of some members of the three-fingered toxin family (Love & Stroud, 1986; Endo & Tamiya, 1987). The molecular models of Fas2 and Fas3, whose crystal structures are not known, were constructed using the residue replacement with the Insight 2.3.0. program. Side chains were then minimized using the Discover program to avoid artificial constraints.

Calculations and display of electrostatic fields

Electrostatic potential fields of the toxins and AChE were determined using the linearized Poisson–Boltzmann equation solved numerically by the DelPhi 2.5 program (Biosym Technologies Inc., 1994). The dielectric constant of water was set to 80, and that of the protein interior to 2. An ionic strength of 0.145 was used. The grid had a spacing of 0.9 Å and overall size of 57.8 Å.

Precollision orientation procedure

The precollision orientation of the fasciculin molecule relative to AChE was calculated using a strategy that considered only electrostatic interactions. Coulombic energies of electrostatic interaction between AChE and Fas1 were calculated by summing the contributions of partial charges of all atoms of these two molecules using the Docking program of Insight 2.3.0 and CFF91 force field. Interactions were measured within short (12 Å) and long (100 Å) range cutoff distances.

The following strategy was used. Five full circles were defined around the center of mass for AChE (Fig. 3). The distance between the mass centers of the two molecules was kept constant at 56 Å, a value consistent with a 20-Å distance as an average shortest distance between AChE and Fas1 molecular surfaces. In local regions where the position was refined, we also used a distance of 10 Å. Each full circle was rotated in 45° incremental positions of Fas1, and the electrostatic interaction energies were calculated (Fig. 8). A zero angle refers to the position directly above an axis aligned down the center of the AChE gorge.

At each of the positions, orientations of Fas1 differing by 90° rotational angles around the respective *x*-, *y*-, and *z*-axes, presuming the tip of the molecule fixed at the zero point (Fig. 8A), were evaluated. The *x* orientation is perpendicular to the average surface of the AChE molecule (Fig. 8B). The overall number of possible orientations of the Fas molecule was 24. These orientations were named by the directions of the orientation of loops II and I (Fig. 8A), presuming the orientation of the loop II always is directly congruent with one of axes. The direction of the orientation of loop I is designated after the direction of

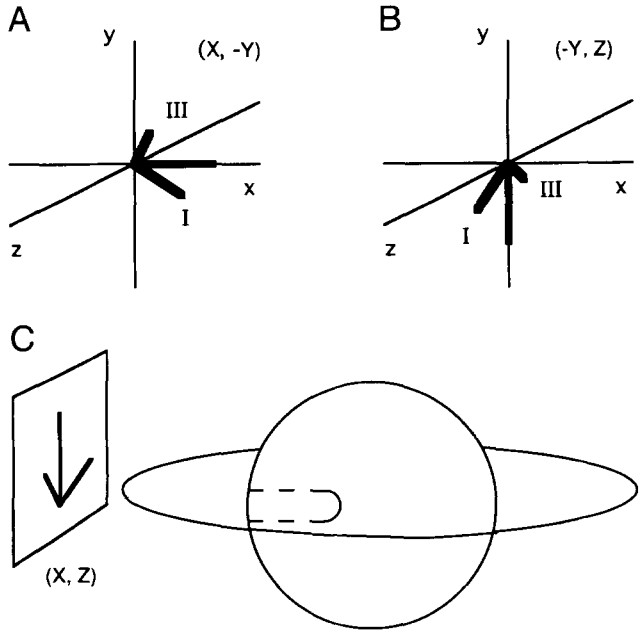

Fig. 8. Precollision orientation of Fasl. **A, B:** Representative examples of orientations of the Fasl molecule used for evaluation of precollision orientations (positions X, Y and $-Y$, Z). Symbols I and III denote structural loops. **C:** Starting position of Fasl (position X, Z) and AChE used in circle 3. Dashed line, position of the gorge.

the vector component associated with this loop that is perpendicular to the direction of the vector of loop II and lies in the same plane as loops I, II, and III. So, for example, orientation X, $-Y$ is the orientation where loop II is directed toward the surface of AChE along the x-axis (Fig. 8A) and loop I is oriented toward the $-Y$ direction. The structure of the Fasl molecule is rigid and rather flat, so the direction of loop III always corresponds to the orientations of loops II and I. Some of orientations were skipped initially due to strong unfavorable electrostatic interaction between AChE and Fasl. We eliminated, for example, positions where the tip of Fas and/or loop III were directed to the surface of AChE (orientations Y, $-X$; $-Y$, $-X$; Z, $-X$). The positions with so-called "flat" orientation, where the largest surface of Fasl is oriented perpendicular to AChE ($-Y$, Z; $-Z$, Y; Z, Y; $-Z$, $-Y$), also had relatively large electrostatic energies and were eliminated. The same situation holds for other orientations. In selected positions of Fasl the energies then were measured at every 6° increment. All of these calculations were made using our own semi-autonomous programs in Insight II. The program kept the AChE molecule stationary while translating the Fasl molecule to each position around AChE and rotating it to the chosen orientation. During the rotation of the Fasl molecule, the axes connecting the mass centers of both molecules were kept at a constant length, and the point of internal rotation of the Fasl molecule was fixed close to its center of mass. With this procedure, the shortest separation distance between the surfaces of molecules varied.

Areas of molecular surfaces that become inaccessible to solvent upon formation of AChE-Fas complexes were calculated using the Solvation 2.5 program (Biosym Technologies, Inc., 1994). In order to define these buried surface areas in the complex, we calculated the solvent-accessible surfaces of the individual molecules and of the complexes. A molecular surface algorithm (Connolly, 1983) with a 1.6-Å radius of probe was used to determine the solvent accessibility of each molecule.

Selection of fasciculin-AChE complexes

In the first selection procedure the area of the buried surface of interaction and its shape complementarity were weighed against the complementarity of electrostatic field vectors of both molecules. For example, complexes with relatively small contact areas were still selected if they had significant complementarity of electric fields, whereas structures with small contact areas and strongly opposing electric field orientations were eliminated.

The topography of residues at the interface was closely evaluated. Complementary groups were aligned to maximize salt bridges and hydrophobic clusters. Complexes with relatively small interfacial areas but significant complementarity of interfacial residues, by virtue of formation of a significant number of salt bridges and hydrophobic clusters, were selected for further investigation.

Each potential complex selected for further investigation was minimized using the Discover 3.1 program (Biosym Technologies, Inc., 1994) in CVFF force field. This afforded an opportunity to adjust the fit of the intermolecular complexes avoiding the problem of "rigid bodies." Using this approach, we avoided rejection of remaining favorable complexes because of artificial van der Waals energy barriers between nonenergy-minimized side chains of both molecules. A cutoff distance of 25 Å was used in these calculations. The peptide backbones of both molecules were constrained during the minimization.

Acknowledgments

We thank Drs. Stanislaw Wlodek, Jan Antosiewicz, at the University of Houston, and Dr. Anatoly Schmidt at Biosym Technologies, Inc. for helpful comments. We also thank Dr. Lynn Ten Eyck at the San Diego Supercomputer Center for his assistance and valuable advice during the course of this study. This work was supported by USPHS grant GM18360 and DAMD 17-91C-1056 to P.T.

References

Brzozowski AM, Derewenda U, Derewenda ZS, Dodson GG, Lawson DM, Turkenburg JP, Bjorkling F, Huge-Jensen B, Patkar SA, Thim L. 1991. A model for interfacial activation in lipases from the structure of a fungal lipase-inhibitor complex. *Nature 351*:491-494.

Cervenansky C, Dajas F, Harvey AL, Karlsson E. 1991. Fasciculins, anticholinesterase toxins from mamba venoms: Biochemistry and pharmacology. In: Harvey AL, ed. *Snake toxins*. New York: Pergamon Press, Inc. pp 303-321.

Cervenansky C, Engstrom A, Karlsson E. 1994. Study of structure-activity relationship of fasciculin by acetylation of amino groups. *Biochim Biophys Acta 1199*:1-5.

Connolly M. 1983. Solvent-accessible surfaces of proteins and nucleic acids. *Science 221*:709-713.

Endo T, Tamiya N. 1987. Current view on the structure-function relationship of postsynaptic neurotoxins from snake venoms. *Pharmacol Ther 34*:403-451.

Endo T, Tamiya N. 1991. Structure-function relationship of postsynaptic neurotoxins from snake venoms. In: Harvey AL, ed. *Snake toxins*. New York: Pergamon Press, Inc. pp 165-222.

Faure G, Boulain JC, Bouet F, Montenay-Garestier T, Fromageot P, Menez A. 1983. Role of indole and amino groups in the structure and function of *Naja nigricolis* toxin alpha. *Biochemistry 22*:2068-2076.

Grochulski P, Li Y, Schrag JD, Cygler M. 1994. Two conformation states of *Candida rugosa* lipase. *Protein Sci 3*:82-91.

Karlsson E, Mbugua PM, Rodriguez-Itthurralde D. 1984. Fasciculins, anticholinesterase toxins from the venom of the green mamba *Dendroaspis angusticeps*. *J Physiol (Paris) 79*:232–240.

Karlsson E, Mbugua PM, Rodriguez-Itthurralde D. 1985. Anticholinesterase toxins. *Pharmacol Ther 30*:259–276.

Kim KS, Lee JY, Lee SJ, Ha TK, Kim DH. 1994. On binding forces between aromatic ring and quaternary ammonium compounds. *J Am Chem Soc 116*:7399–3400.

le Du MH, Marchot P, Bougis PE, Fontecilla-Camps JC. 1992. 1.9-Å resolution structure of fasciculin 1, an anti-cholinesterase toxin from green mamba snake venom. *J Biol Chem 267*:22122–22130.

Love R, Stroud R. 1986. The crystal structure of α-bungarotoxin at 2.5 Å resolution: Relation to solution structure and binding to acetylcholine receptor. *Protein Eng 1*:37–46.

Marchot P, Khelif A, Ji YH, Mansuelle P, Bougis PE. 1993. Binding of ^{125}I-fasciculin to rat brain acetylcholinesterase. The complex still binds diisopropyl fluorophosphate. *J Biol Chem 268*:12458–12467.

Martin BM, Chibber BA, Maelicke A. 1983. The sites of neurotoxicity in α-cobratoxin. *J Biol Chem 258*:8714–8722.

Ollis DL, Cheah E, Cygler M, Dijkstia B, Frolow F, Franken SM, Harel M, Remington SJ, Silman I, Schrag JD, Sussman JL, Vercheuren KHG, Goldman A. 1992. The α,β hydrolase fold. *Protein Eng 5*:197–211.

Pillet L, Tremeau O, Ducancel F, Drevet P, Zinn-Justin S, Pinkasfeld S, Boulain JC, Menez A. 1993. Genetic engineering of snake toxins. *J Biol Chem 268*:909–916.

Radić Z, Duran R, Vellom D, Li Y, Cervenansky C, Taylor P. 1994. Site of fasciculin interaction with acetylcholinesterase. *J Biol Chem 269*:11233–11239.

Radić Z, Gibney G, Kawamoto S, MacPhee-Quigley K, Bongiorno C, Taylor P. 1992. Expression of recombinant acetylcholinesterase in a baculovirus system: Kinetic properties of glutamate 199 mutants. *Biochemistry 31*: 9760–9767.

Rees B, Bilwes A, Samana J, Moras D. 1990. Cardiotoxin V_4^{II} from *Naja mossambica*, the refined crystal structure. *J Mol Biol 214*:281–297.

Ripoll D, Faerman C, Axelsen P, Silman I, Sussman J. 1993. An electrostatic mechanism for substrate guidance down the aromatic gorge of acetylcholinesterase. *Proc Natl Acad Sci USA 90*:5128–5132.

Shafferman A, Ordentlich A, Barak D, Kriman C, Ber R, Bino T, Ariel N, Osman R, Velan B. 1994. Electrostatic attraction by surface charge does not contribute to the catalytic efficiency of acetylcholinesterase. *EMBO J 13*:34448–34455.

Smith JL, Corfield PWR, Hendrickson WA, Low BW. 1988. Refinement at 1.4 Å resolution of a model of erabutoxin *b*. Treatment of ordered solvent and discrete disorder. *Acta Crystallogr A 44*:357–368.

Sussman JL, Harel M, Frolow F, Oefner C, Goldman A, Toker L, Silman I. 1991. Atomic structure of acetylcholinesterase from *Torpedo californica*: A prototypic acetylcholine-binding protein. *Science 253*:872–879.

Tan R, Truong T, McCammon J, Sussman J. 1993. Acetylcholinesterase: Electrostatic steering increases the rate of ligand binding. *Biochemistry 32*:401–403.

Taylor P, Lappi S. 1975. Interaction of fluorescence probes with acetylcholinesterase. The site and specificity of propidium binding. *Biochemistry 14*:1989–1997.

Walkinshaw MD, Saenger W, Maelicke A. 1980. Three-dimensional structure of the "long" neurotoxin from cobra venom. *Proc Natl Acad Sci USA 77*:2400–2404.